



UNIVERSITY OF LEEDS

This is a repository copy of *Fullerene up-take alters bilayer structure and elasticity: A small angle X-ray study.*

White Rose Research Online URL for this paper:
<http://eprints.whiterose.ac.uk/85150/>

Version: Accepted Version

Article:

Drasler, B, Drobne, D, Sadeghpour, A orcid.org/0000-0002-0475-7858 et al. (1 more author) (2015) Fullerene up-take alters bilayer structure and elasticity: A small angle X-ray study. *Chemistry and Physics of Lipids*, 188. pp. 46-53. ISSN 0009-3084

<https://doi.org/10.1016/j.chemphyslip.2015.04.001>

© 2015, Elsevier. Licensed under the Creative Commons Attribution-NonCommercial-NoDerivatives 4.0 International
<http://creativecommons.org/licenses/by-nc-nd/4.0/>

Reuse

Items deposited in White Rose Research Online are protected by copyright, with all rights reserved unless indicated otherwise. They may be downloaded and/or printed for private study, or other acts as permitted by national copyright laws. The publisher or other rights holders may allow further reproduction and re-use of the full text version. This is indicated by the licence information on the White Rose Research Online record for the item.

Takedown

If you consider content in White Rose Research Online to be in breach of UK law, please notify us by emailing eprints@whiterose.ac.uk including the URL of the record and the reason for the withdrawal request.



eprints@whiterose.ac.uk
<https://eprints.whiterose.ac.uk/>

Fullerene Up-Take Alters Bilayer Structure and Elasticity: A Small Angle X-ray Study

Barbara Drasler^a, Damjana Drobne^{a}, Amin Sadeghpour^b, Michael Rappolt^{b**}*

^a Department of Biology, Biotechnical Faculty, University of Ljubljana, Vecna pot 111, 1000 Ljubljana, Slovenia

^b School of Food Science & Nutrition, University of Leeds, Leeds, LS2 9JT, UK

Keywords: Fullerene, toxicity, POPC, bilayer structure, membrane undulations, SAXS

Corresponding authors:

*Damjana Drobne, Department of Biology, Biotechnical Faculty, University of Ljubljana, Vecna pot 111, 1000 Ljubljana, Slovenia; Tel: +3861 3203375; E-mail: damjana.drobne@bf.uni-lj.si

**Michael Rappolt, School of Food Science & Nutrition, University of Leeds, Leeds, LS2 9JT, UK. Tel: +44(0)113 3431931; E-mail: m.rappolt@leeds.ac.uk

Abstract

The coupling of fullerene (C_{60}) to the structure and elasticity of 1-palmitoyl-2-oleoyl-*sn*-glycero-3-phosphocholine bilayers has been explored by synchrotron small angle X-ray scattering. Multilamellar vesicles were loaded with 0, 2 and 10 mol. % of C_{60} and studied in a temperature range from 15-65 °C. The addition of C_{60} caused an increase in the bilayer undulations (~20 %), in the bilayer separation (~15%), in the linear expansion coefficient and caused a drop in the bending rigidity of the bilayers (20-40 %). Possible damaging effects of fullerene on biomembranes are mainly discussed on the basis of altered bilayer fluidity and elasticity changes.

1. Introduction

Fullerenes C_{60} are one of the most studied carbon nanomaterials due to their extraordinary material properties comprising their small size, spherical geometry, hydrophobicity, electronic configurations and photo-excitation states (Bakry et al., 2007). Moreover, the possibility for derivatization and functionalization makes fullerene a highly attractive material for various applications. In particular their carbon-based cage structure with delocalized π -molecular orbital electrons and diameter of about 1 nm makes them a promising candidate for medical diagnostic or therapeutic agents by entrapping desired material in the cage (Dellinger et al., 2013). Due to their unique structure and strong electronic properties, fullerenes C_{60} can also be used as radical scavengers, antioxidants, antiviral agents or enzyme inhibitors (Bakry et al., 2007; Dellinger et al., 2013; Rossi et al., 2013). Furthermore, the group of Ikeda successfully introduced the use of liposomes as solvents for fullerenes in order to deliver them into cells (Ikeda et al., 2012).

On the other hand the unique characteristic of C_{60} can also provoke undesired biological effects (Sayes et al., 2004; Sayes et al., 2005). In a recent review, Rossi et al. (2013) pointed out that lipid membranes most likely mediate a mechanism of fullerene toxicity. There is still no clear consensus on the cytotoxicity of C_{60} , but is presumably related to biomembrane structure and functionality (Dellinger et al., 2013). In order to guarantee efficient and safe applications of C_{60} , it is of paramount importance that C_{60} -membrane interactions get understood (Monticelli et al., 2009; Rossi et al., 2013).

Computer simulation studies demonstrated that C_{60} may provoke formation of micropores or holes in phospholipid membranes, which then would contribute to membrane leakage (Chang and Lee, 2010; Qiao et al., 2007; Monticelli et al., 2009). Larger aggregates of C_{60} adhere on the surface of the bilayer membrane, whereas individual C_{60} molecules or small nano-agglomerates can penetrate into the lipid bilayer by means of passive transport through transient micropores in the membrane (Bedrov et al., 2008; Qiao et al., 2007). Once incorporated in the membrane, various studies specify that fullerenes are homogeneously dispersed in the centre of the bilayer membrane (within a 1-2 nm regime) (Li et al., 2008; Qiao et al., 2007; Wong-Ekkabut et al., 2008), and it is commonly anticipated that this incorporation causes an overall thickening of the membrane. Wong-Ekkabut et al. (2008) have additionally shown that a slight bilayer thickness increase is accompanied by a quite significant softening of the membrane. However, in their studies no bilayer rupture, micellization or formation of pores was seen, and they conclude that fullerene toxicity cannot

be attributed to mechanical damage of the membrane alone, but elastic property changes of the bilayer have also to be taken into account.

Spectroscopy studies (Bensasson et al., 1994; Hungerbuehler et al., 1993) provided first experimental evidence on successful incorporation of C₆₀ fullerenes into vesicular and micellar membranes in aqueous environment. More recently, investigations on phospholipid model membranes have shown that both pristine and water soluble derivatives of C₆₀ not only induce changes in the structural and elastic properties of the lipid bilayer, but also do change the phase behaviour (Chen and Bothun, 2009; De Maria et al., 2006; Jeng et al., 2003; Jeng et al., 2005). Based on both, experimental and simulation studies, it has been further predicted that the partitioning of fullerene into lipid membranes is thermodynamically highly favourable (over $30k_B T$) (Rossi et al., 2013). We note though that the hydrophilic addends of functionalized C₆₀ have a strong tendency to intercalate into the phospholipid bilayer keeping the C₆₀s attached to the membrane interface, whereas pristine C₆₀ molecules, when solubilized in the liposomal POPC bilayers, tend to aggregate in the bilayer interior and cause strong reorganization of the phospholipid bilayer chains (De Maria et al., 2006).

In vitro studies revealed that nanoscale aggregates of water soluble C₆₀ derivatives caused cellular damage, which was provoked through lipid peroxidation (Sayes et al., 2005). On the other hand, the protection of lipid membranes from radical induced-lipid peroxidation was found to be higher with pristine, liposoluble C₆₀, than its water soluble derivatives (Wang et al., 1999). Thus, fullerene's toxicity depends on the type and degree of functionalization; it has been shown that toxicity is seven orders of magnitude higher with pristine fullerenes in comparison to highly soluble functionalized derivatives (Sayes et al., 2004). When interpreting results of both *in vitro* studies, and studies on model membrane systems, it is therefore important to keep in mind the different behaviour of pristine fullerene C₆₀ as compared to diverse fullerene derivatives.

In our previous study, we demonstrated by small angle X-ray scattering (SAXS) measurements that the up-take of fullerene-aggregates has the potential to disturb significantly the integrity of 1-palmitoyl-2-oleoyl-*sn*-glycero-3-phosphocholine (POPC) liposomes. In this case, the up-take of fullerene-aggregates (or smaller nano-agglomerates) from the aqueous phase was induced by several freeze and thaw cycles between room and liquid nitrogen temperature. Without destroying the integrity of the liposomes (no freeze and thawing applied), the fullerene-aggregates adhere to the outside of the vesicles and stabilize them, as observed in the increased stacking order of the bilayers (Zupanc et al., 2012). This

latter observation is in agreement with De Maria et al. (2006), who also suggested that the presence of C_{60} increases the stability of POPC liposomes.

The aim of this study was to experimentally assess the interactions between fully dissolved pristine C_{60} and POPC multilamellar vesicles (MLVs) (no remaining C_{60} clusters in the excess of water phase). We explored their temperature dependent interaction by synchrotron SAXS. Our results are presented with respect to (i) the observed structural changes of the bilayer, and (ii) to the determined bilayer separation and membrane fluctuations, (iii) followed by a discussion on changes of the membrane elasticity. (iv) A comparison with the outcome on other model membrane systems is given, and (v) finally we discuss different scenarios for the interaction of fullerenes with biomembranes.

2. Materials and methods

2.1 Sample preparation

A stock solution of C₆₀ nanoparticles (black crystalline powder, with estimated nominal purity >99.5 %, Sigma-Aldrich, Steinheim, Germany) in chloroform (CHCl₃; Merck KGaA, Darmstadt, Germany) was prepared with a final concentration of 0.16 g/L. This is the solubility limit of C₆₀ in chloroform at room temperature (Ruoff et al., 1993) and complete solubility was obtained by using 4 mg of powder C₆₀ in 25 mL of CHCl₃ and applying water bath sonication for 3 h at 30 °C (note, after sonication the suspension appears clear and purple; even after 12 hours the entire solution remains transparent clearly precluding the existence of aggregates, which would otherwise accumulate as sediment). A lipid stock solution was prepared by dissolving POPC powder (1-palmitoyl-2-oleoyl-*sn*-glycero-3-phosphocholine, Avanti Polar Lipids, Inc., Alabaster, AL, USA) in CHCl₃ (50 mg POPC/mL). The pure POPC (control) as well as the POPC samples with 2 and 10 mol. % of C₆₀, respectively, were prepared from appropriately weighted amounts of the stock solutions (C₆₀ mol. % := C₆₀ moles / (C₆₀ moles plus POPC moles) · 100). After solvent (CHCl₃) evaporation for 12 h under vacuum conditions, MLVs were prepared by rehydrating the dry thin films with 0.1 mL of distilled water and subsequent vortexing of the dispersions was applied (each sample was vortexed intermittently five times at room temperature for 2 min). The readily prepared dispersions were subjected to a light stream of nitrogen and stored at -20 °C in sealed vials until usage **for several days (note, no signs of C₆₀ sediment in the form of black deposit on the bottom of the recipients was observed).**

2.2 Small angle X-ray scattering experiments

Temperature resolved small angle X-ray scattering (SAXS) experiments were carried out at the Austrian SAXS beamline situated at the Synchrotron Trieste, Italy (Amenitsch et al., 1998; Bernstorff et al., 1998), using a wavelength of $\lambda = 1.54 \text{ \AA}$. Diffraction profiles were detected utilizing a Mar300 image-plate detector (Marresearch GmbH, Norderstedt, Germany) and calibrated using a powder sample of silver behenate (CH₃(CH₂)₂O-COOAg; *d*-spacing 58.38 Å) (Huang et al., 1993). The lipid dispersions were measured in a thin-walled 1 mm diameter quartz capillary in a steel cuvette (Anton Paar, Graz, Austria), which was inserted into a brass block. This sample holder block was in thermal contact with a water circuit, i.e., it was connected to a water bath with a freely programmable control unit (Unistat CC, Huber, Offenburg, Germany). In order to avoid air convection at the capillary the

entrance and exit windows of the block have been covered with a thin polymer film. The temperature was measured in the vicinity of the capillary in the sample holder block with a Pt-element (100 Ω). Prior to measurement each sample was equilibrated for a minimum of 10 min at a predetermined temperature with an uncertainty of ± 0.1 $^{\circ}\text{C}$. The exposure time was set to 120 s. Scattering patterns were integrated using the program *FIT2D* (Hammersley, 1997). Background scattering originating from water, the capillary and air was subtracted, and data sets were normalized using the transmitted intensity, which was measured by a photodiode placed in the beamstop. Background corrected SAXS patterns were analysed by the application of the modified Caillé theory (see Supplementary material). The technique and underlying premises have been described previously in detail (Pabst et al., 2003; Pabst et al., 2000b; for a review see Rappolt and Pabst, 2008)). The bilayer model used and its applications have been presented elsewhere (Rappolt, 2010). From the fits to the scattered intensities $I = S(q)|F(q)|^2/q^2$ ($S(q)$: structure factor; $F(q)$: form factor) we directly obtained the lamellar repeat distance d and the headgroup-to-headgroup thickness, d_{HH} . The bending fluctuation or Caillé parameter (Caillé, 1972; Zhang et al., 1994),

$$\eta = \frac{\pi k_B T}{2d^2 \sqrt{K_C B}} \quad (1)$$

was directly obtained from the fits and depends on the membrane bending rigidity, K_C , and the bulk compression modulus, B (De Gennes and Prost, 1993).

3. Results and Discussion

3.1 Structural Changes in the Bilayer

Small angle X-ray scattering experiments were carried on MLVs of POPC dispersed in distilled water (dH₂O) and used as a model membrane system to investigate the influence of the incorporation of C₆₀. In Fig. 1 typical diffraction patterns are shown for samples recorded at room temperature (See Supplementary material). All SAXS pattern were globally fitted allowing the extraction of both structural and mechanical data of the membranes.

Authors' remark: Please insert Fig. 1 here.

POPC bilayers alone have been thoroughly studied and analysed, both under constant temperature and rapid heating conditions (Pabst et al., 2000a; Pabst et al., 2000b; Rappolt et al., 2004; Rappolt and Pabst, 2008). The displayed structural behavior in the temperature range from 15 to 65 °C compares well to literature results (Fig. 2, red circles). While the membrane thickness decreases monotonously with increasing temperature, the water layer thickness increases. Both trends are readily understood: First, increasing temperature leads to a rise of the *trans* to *gauche* rotamers' ratio in the hydrocarbon chains, which in turn leads to lipid chain shortening (Seelig and Seelig, 1974). Second, due to a membrane softening the undulations of the bilayers enhance with increasing temperature and cause additional repulsion of adjacent bilayers (Pabst et al., 2003).

Authors' remark: Please insert Fig. 2 here.

The incorporation of C₆₀ in the POPC bilayers clearly displays bigger *d*-spacing as compared to the pure lipid/water system (Fig. 2A). The question is what causes the bigger lattice spacings? Having applied a global fitting procedure based on the second type of lattice disorder description by Caillé (see Supplementary material, Caillé, 1972; Pabst et al., 2000b) the lattice parameter can be divided into its hydrophobic and hydrophilic sub-compartments, i.e., into the head-to-headgroup thickness, d_{HH} , and the free water layer thickness, d_W , that we define in this study as $d - d_{HH} - d_H$ (for sake of simplicity we estimate the headgroup extension, d_H , to be equal to 1.0 nm (McIntosh and Simon, 1986)). A closer look onto these structural parameters reveals mainly two effects. First, the membrane thickness, d_{HH} , does not alter much with respect to the unloaded membranes (Fig. 2B). In the temperature range from 15 to 35 °C the membrane thicknesses of the POPC/C₆₀ bilayers are only slightly smaller, while from 45 to 65 °C the membrane thicknesses are practically the same (Fig. 2B). Nevertheless, there is a systematic increase in the linear thermal expansion coefficient, α ,

$$\alpha = \frac{\Delta d_{HH}}{d_{HH} \cdot \Delta T} \quad (2)$$

with increasing fullerene content. The averaged linear thermal expansion coefficient is $2.6 \times 10^{-3} \text{ }^\circ\text{C}^{-1}$ for pure POPC bilayers, which compares well to published values of $\alpha = 2.2 \times 10^{-3} \text{ }^\circ\text{C}^{-1}$ for POPC below $50 \text{ }^\circ\text{C}$ (Pabst et al., 2000a) and is close to the dipalmitoyl-phosphatidylcholine (DPPC) value of $2.50 \times 10^{-3} \text{ }^\circ\text{C}^{-1}$ (Seelig and Seelig, 1974). In the presence of 2 mol. % of C_{60} the thermal expansion coefficient increases to $1.65 \times 10^{-3} \text{ }^\circ\text{C}^{-1}$, and adding 10 mol. % of C_{60} $\alpha = 1.50 \times 10^{-3} \text{ }^\circ\text{C}^{-1}$ (note, the magnitude of α decreases). Briefly, in the presence of fullerenes the bilayer thickness does not change much in the studied temperature interval (changes in d_{HH} occur in the range of 0.16 to +0.08 nm), however, the linear thermal expansion coefficient increases quite substantially (60 %). At lower temperatures the presence of fullerenes induces a relatively higher *gauche/trans* ratio in the hydrocarbon chains (seen in the smaller bilayer thickness), and at higher temperatures ($> 55 \text{ }^\circ\text{C}$) the induction of additional rotamers is hampered (seen in the slightly bigger bilayer thickness). Thus, we assume that the presence of C_{60} in the hydrophobic core of the bilayers provokes, to some extent, disorder in the lipid chains in order to accommodate the presence of the C_{60} , whereas at higher temperatures greater numbers of *gauche* conformations per lipid chain are most probably hindered by the van der Waals interactions between lipid chains and fullerenes, i.e. the overall chain fluidity profile is altered.

3.2 Bilayer Separation and Membrane Fluctuations

Secondly, in the presence of C_{60} the inter-membrane distance or the free water layer thickness, d_w , increases up to 15 % (+ 0.21 nm) as compared to the pure POPC/water system (Fig. 2C). Most probably the cause lies in the greater mean fluctuations of the membrane separations that we observed (Fig. 2D). The Caillé parameter, η (eq. 1) translates into mean fluctuation of inter-membrane distance, σ , by the relation (Petrache et al., 1998)

$$\sigma = \sqrt{\eta} \cdot \frac{d}{\pi} \quad (3)$$

Authors' remark: Please insert Fig. 3 here.

These fluctuations monotonously increase with temperature from 0.47 to 0.68 nm for the pure POPC system and from 0.54 to 0.76 nm for POPC bilayers with 10 mol. % of C_{60} (referring to the data of Fig. 2D). Thus, the incorporation of C_{60} intensifies σ in the range of 15-35 %. In Fig. 3 the mean fluctuation of inter-membrane distances is plotted as function of C_{60}

concentration for the data recorded at room temperature. Note, a monotonous increase of σ with fullerene concentration is observed over the whole temperature range (15 – 65 °C).

3.3 Bending Rigidity Modulus versus Bulk Compression Modulus

The interpretation of the above observations is briefly outlined as follows: For larger bilayer separations ($d_w > 1$ nm) Helfrich (1978) proved the occurrence of a repulsive force for bilayers which are flexible enough to perform out-of-plane undulations. Considering only steric interactions caused by collision of bilayers, this steric free energy is inversely proportional to the membrane bending rigidity, K_C and to the squared bilayer separation ($K_C^{-1} d_w^{-2}$). However, the bending rigidity, K_C , is not directly accessible by our SAXS data, since the experimental Caillé parameter η depends on both, K_C and on the bulk compression modulus, B (cf. eq. 1). Nevertheless, it is instructive to estimate the order of magnitude of possible changes for K_C . Under the assumption that the bulk compression modulus observed for dimyristoyl-phosphatidylcholine (DMPC) (Pabst et al., 2003) ($B = 8 \times 10^{13}$ J/m⁴ from $T = 25$ to 35°C) is similar to the one of POPC, we find that K_C for pure POPC bilayers monotonously decreases in the temperature interval from 15 °C to 65 °C from 10 to 3×10^{-20} J (this compares well with literature values reviewed in Rappolt and Pabst, 2008). Using the same estimate for B also for the 10 mol. % of C₆₀/POPC data, the bending rigidity decreases monotonously from 6 to 2×10^{-20} J. This means for instance that at 25 °C the addition of 10 mol. % of C₆₀ causes a drop of K_C of about 4×10^{-20} J. This trend compares very well with the computer simulation study of Wong-Ekkabut et al. (2008), who determined a drop of K_C in dioleoyl-PC bilayers from 5.5×10^{-20} J to 4.4×10^{-20} J in the presence of 11 mol. % of C₆₀. We note that the drop of the bending rigidity in the simulated model is not as drastic as in our estimation (1×10^{-20} compared to 4×10^{-20} J), however, our estimation for K_C in the presence of fullerenes displays a lower limit, since we did not consider a change of the bulk compression modulus, B . Assuming that the measured increase in the mean fluctuation of inter-membrane distances σ (Fig. 3) is additionally caused by a drop in B , would actually lead to greater K_C values. In any case, our experimental data provide strong evidence that the presence of fullerene renders the bilayers more flexible, and in turn demonstrates that the steric free energy, f_U , can increase quite significantly.

3.4 Interactions of Fullerenes with Different Model Membranes

The X-ray data analysis summarized in Fig. 4 illustrates that the fullerenes accumulate in the hydrophobic core of the bilayers and alter the nanostructural response of the bilayers to temperature. This is evident, since any significant accumulation of C₆₀ in the headgroup region would have led to a reduction in the headgroup density, which is not observed (left hand side in Fig. 4). The position of the fullerenes centred around the methylene trough region was also seen in grazing incidence measurements on dipalmitoyl-PC films kept at 28 °C under relative humidity conditions of 50 % (Jeng et al., 2005), observed by differential scanning calorimetry measurements combined by ¹³C NMR (Ikeda et al., 2011) in dimyristoyl-PC vesicles, concluded from cryogenic transmission electron microscopy on the formation of bicelles (Ikeda et al., 2014) (binary and ternary lipid mixtures were applied), and further supported in various simulation studies (Bedrov et al., 2008; Li et al., 2007; Shinoda et al., 2012; Wong-Ekkabut et al., 2008). Recently also the energetics of C₆₀ permeation validated with computational all-atom model of fullerene (Monticelli, 2012), demonstrate that the up-take of fullerenes into the membrane interior is thermodynamically favoured, and a molecular dynamics study highlighted the “barrierless” passive transport of C₆₀ from the aqueous phase into the membranes (Bedrov et al., 2008). Interestingly, not only the free energy decreases as the fullerene passes from bulk water into the hydrophobic core of the membrane, but more precisely, the drop in the free energy is due to stronger van der Waals interactions between the fullerenes and the lipids, rather than driven by hydrophobic interactions. This supports our findings that the presence of fullerenes decreases the rate of induced *trans* to *gauche* conformations at higher temperatures (see above discussion on the linear thermal expansion coefficient).

Authors' remark: Please insert Fig. 4 here.

A broad consensus has been reached that fullerenes accumulate in the hydrophobic core of lipid bilayers, and moreover, are highly soluble in PC-bilayers. A maximum molar ratio of 30% fullerene to lipid could be obtained experimentally (Ikeda et al., 2012), and this high solubility was further confirmed by simulation studies on POPC model membranes (Barnoud et al., 2014). **The fullerenes in POPC bilayers were simulated to be largely monomeric, even when reaching such large C₆₀/lipid ratios.** Interestingly, the hydrocarbon chain density and the perturbation of chain to chain interactions are the key factors explaining such high C₆₀-solvation capacities of PC-bilayers. Nevertheless, the scientific debate is still open to which extent fullerenes aggregate within the bilayer. Simulations carried out by Wong-

Ekkabut et al. (2008) do not display stable aggregates of C₆₀, which is in agreement with other atomistic simulations showing that interactions between fullerenes in lipid bilayers are repulsive at short distances (Li et al., 2007). However, other simulation studies predict stable aggregations of C₆₀ in the centre of the lipid bilayer (Shinoda et al., 2012), and also the formation of bicelles at low lipid concentration has been interpreted to be stabilized by the stable aggregation of fullerenes C₇₀ (Ikeda et al., 2014). The latter understanding would also mean that at least locally, the membrane rigidity is expected to increase throughout the extended areas of C₆₀ aggregates. However, the X-ray data of this work does not support this notion. All diffraction patterns, both at 2 and 10 mol. % of C₆₀ display flawlessly sharp Bragg peaks without any visible shoulders (see Fig.1 and Supplementary material) indicating a single lamellar phase rather than the existence of two coexisting lamellar phases, one being rich in C₆₀ and the other being nearly deprived from C₆₀, i.e. the latter resembling practically a pure fluid lamellar phase. Noteworthy, there are plenty of examples in literature for phase separated lamellar phases observed on MLVs, but in all cases clearly distinct lattices are observed (Hodzic et al., 2008; Rappolt and Rapp, 1996). Nevertheless, smaller aggregates of fullerenes and/or transient short living clusters would be consistent with our SAXS data. Additionally we have recently shown (Zupanc et al., 2012) that as long as fullerenes, which rapidly aggregate in water, stick to the outside of MLVs (Fig. 5A), these adherent aggregates improve the inner stacking order of the fluid lamellar phase. We observed both a reduction in the Caillé parameter, i.e. a decrease in membrane fluctuations and a concomitant increase in the quasi long range order (the diffraction peaks got sharper), when the fullerene clusters (smaller agglomerates and aggregates) adhered to the MLVs. We like to point out, that different aggregation states might be another source of conflicting experimental interpretations, because bigger aggregates of C₆₀ adhering to the outside of the membranes increase the bilayer's rigidity, whereas perfectly dissolved fullerenes in the hydrophobic interior of the bilayers (Fig. 5B) decrease the bending rigidity.

Authors' remark: Please insert Fig. 5 here.

3.5 Scenarios for the Interaction of Fullerenes with the Lipid Matrix of Biomembranes

Based on our experimental data, we discuss in the following the general influence of fullerenes on the lipid matrix of biomembranes. Consequently, three possible damaging effects of fully dissolved fullerenes in biomembranes can be imagined: (i) altered fluidity of the bilayer may change the functionality of the biomembrane (e.g. endo- and exocytose

processes; compare section 3.1), (ii) fullerenes may sterically disturb embedded membrane proteins especially in the hydrophobic core region of the bilayer (e.g. during the formation of protein complexes; compare section 3.4), and (iii) expected changes in the lateral pressure profile of membranes may influence negatively the function of embedded membrane proteins (e.g. the opening and closing probability of membrane pores can get altered (Jerebek et al., 2010)).

The influence of the lipid bilayer on membrane protein function is very complex. Gruner (1985) and Cantor (1999; 2002) pointed out that it is possible to couple mechanically the protein activity to the lateral pressure profile of the membrane. Essentially, there are three regimes to be discerned. In the headgroup region repulsions are mainly caused by electrostatic and entropic effects, at the polar/apolar interface the hydrophobic effect leads to a strong lateral attraction and last mutual repulsion of hydrocarbon chains determine the lateral pressure profile in the hydrophobic core region. Hence, the fullerene incorporation into phospholipid membranes is expected to mainly alter the pressure profile in the centre of the membrane, i.e. augmenting van der Waals interactions between the fullerenes and the lipids leads to a decrease of the pressure in the lipid chain region. Changes in the lateral pressure will alter the dynamics of membrane proteins and thus their activity, however, to what extent remains speculation, and further simulation studies on the lateral pressure profile in the presence and absence of fullerenes are necessary to detail the mechanic bilayer impact on embedded proteins.

Last we point out that the hydrophobic thickness of the bilayers does not alter much under the presence of C_{60} (this work and Jeng et al., 2005). Therefore the energetic cost of adapting the bilayer hydrophobic thickness to match the hydrophobic length of membrane proteins, will not be altered much by the hydrophobic mismatch (Lundbaek et al., 2010), but rather be influenced by stronger changes in the elastic moduli of the membrane. For instance in the presence of about 10 mol. % of C_{60} in the interior of bilayers an expected drop in the bending rigidity K_C in the order of 20-40 % is expected (Wong-Ekkabut et al., 2008), and would consequently lead to a decrease in the free energy associated with bilayer deformations occurring in the boundary regions of the membrane with embedded proteins (Lundbaek et al., 2010).

4. Conclusion

Our SAXS data on POPC model membranes show that fullerenes accumulate in the hydrophobic core of the bilayers without any sign of aggregation up to 10 mol. % of C₆₀. We further provide experimental evidence that the fullerene incorporation into biomembranes will lead to various subtle structural and more prominent mechanical changes of the bilayer matrix. As pointed out also by other groups (Wong-Ekkabut et al., 2008), already changes in biomembrane elasticity alone (which depends on membrane composition) can alter activity of some membrane proteins and change membrane functioning, without the need for significant membrane disruptions. While we could clearly demonstrate that the C₆₀ incorporation increases the bilayer's elasticity quite significantly, it still remains a matter of further research whether these alterations are sufficient to explain the C₆₀ nanotoxicity.

Acknowledgements

This work was carried out at Elettra Synchrotron facilities (Trieste, Italy), under proposal agreement No 20120224. The authors gratefully acknowledge the collaboration with Austrian SAXS Beamline (Institute of Inorganic Chemistry, Graz University of Technology c/o Sincrotrone Trieste, Italy). This project has also received funding from the Slovenian Research Agency (ARRS) under Grant Agreement No J1-4109. This work was also supported by the Ministry of Education, Science, Culture and Sport of Republic of Slovenia under a grant "Innovative scheme of co-funding doctoral studies promoting co-operation with the economy and solving of contemporary social challenges" under Grant No 160-21. The authors would like to thank Barbara Sartori, Veno Kononenko, Martin Šimon and Sabina Boljte for their technical assistance.

References

- Amenitsch, H., Rappolt, M., Kriechbaum, M., Mio, H., Laggner, P., Bernstorff, S., 1998. First performance assessment of the small-angle X-ray scattering beamline at ELETTRA. *J Synchrotron Rad.* 5, 506-508.
- Bakry, R., Vallant, R.M., Najam-Ul-Haq, M., Rainer, M., Szabo, Z., Huck, C.W., Bonn, G.K., 2007. Medicinal applications of fullerenes. *International Journal of Nanomedicine* 2, 639-649.
- Barnoud, J., Rossi, G., Monticelli, L., 2014. Lipid Membranes as Solvents for Carbon Nanoparticles. *Physical Review Letters* 112, **068102**.
- Bedrov, D., Smith, G.D., Davande, H., Li, L.W., 2008. Passive transport of C-60 fullerenes through a lipid membrane: A molecular dynamics simulation study. *Journal of Physical Chemistry B* 112, 2078-2084.
- Bensasson, R.V., Bienvenue, E., Dellinger, M., Leach, S., Seta, P., 1994. C60 in Model Biological Systems. A Visible-UV Absorption Study of Solvent-Dependent Parameters and Solute Aggregation. *Journal of Physical Chemistry* 98, 3492-3500.
- Bernstorff, S., Amenitsch, H., Laggner, P., 1998. High-throughput asymmetric double-crystal monochromator of the SAXS beamline at ELETTRA. *Journal of Synchrotron Radiation* 5, 1215-1221.
- Caillé, A., 1972. Remarques sur la diffusion des rayons X dans les smectiques A. *C.R.Acad.Sc.Paris B* 274, 891-893.
- Cantor, R.S., 1999. Lipid composition and the lateral pressure profile in bilayers. *Biophysical Journal* 76, 2625-2639.
- Cantor, R.S., 2002. Size distribution of barrel-stave aggregates of membrane peptides: influence of the bilayer lateral pressure profile. *Biophys.J.* 82, 2520-2525.
- Chang, R., Lee, J., 2010. Dynamics of C-60 Molecules in Biological Membranes: Computer Simulation Studies. *Bulletin of the Korean Chemical Society* 31, 3195-3200.
- Chen, Y.J., Bothun, G.D., 2009. Lipid-Assisted Formation and Dispersion of Aqueous and Bilayer-Embedded Nano-C-60. *Langmuir* 25, 4875-4879.
- De Gennes, P.G., Prost, J., 1993. *The physics of liquid crystals*, 2nd edition ed. Oxford University Press, Oxford.
- De Maria, P., Fontana, A., Gasbarri, C., Velluto, D., 2006. Effects of fullerene guests on the stability of 1-palmitoyl-2-oleoylphosphatidylcholine liposomes. *Soft Matter* 2, 595-602.
- Dellinger, A., Zhou, Z., Connor, J., Madhankumar, A.B., Pamujula, S., Sayes, C.M., Kepley, C.L., 2013. Application of fullerenes in nanomedicine: an update. *Nanomedicine* 8, 1191-1208.
- Gruner, S.M., 1985. Intrinsic curvature hypothesis for biomembrane lipid composition: a role for nonbilayer lipids. *Proc.Natl.Acad.Sci.U.S.A* 82, 3665-3669.
- Hammersley, R.P., 1997. Fit2d: an introduction and overview. *ESRF Internal Report ESRF97HA02T*.
- Helfrich, W., 1978. Steric Interaction of Fluid Membranes in Multilayer Systems. *Z.Naturforsch.* 33a, 305-315.
- Hodzic, A., Rappolt, M., Amenitsch, H., Laggner, P., Pabst, G., 2008. Differential modulation of membrane structure and fluctuations by plant sterols and cholesterol. *Biophysical Journal* 94, 3935-3944.
- Huang, T.C., Toraya, H., Blanton, T.N., Wu, Y., 1993. X-ray powder diffraction analysis of silver behenate, a possible low-angle diffraction standard. *Journal of Applied Crystallography* 26, 180-184.

- Hungerbühler, H., Guldi, D.M., Asmus, K.D., 1993. Incorporation of C60 into artificial lipid membranes. *Journal of the American Chemical Society* 115, 3386-3387.
- Ikeda, A., Kiguchi, K., Hida, T., Yasuhara, K., Nobusawa, K., Akiyama, M., Shinoda, W., 2014. [70]Fullerenes Assist the Formation of Phospholipid Bicelles at Low Lipid Concentrations. *Langmuir* 30, 12315-12320.
- Ikeda, A., Kiguchi, K., Shigematsu, T., Nobusawa, K., Kikuchi, J.-i., Akiyama, M., 2011. Location of [60]fullerene incorporation in lipid membranes. *Chemical Communications* 47, 12095-12097.
- Ikeda, A., Mori, M., Kiguchi, K., Yasuhara, K., Kikuchi, J., Nobusawa, K., Akiyama, M., Hashizume, M., Ogawa, T., Takeya, T., 2012. Advantages and Potential of Lipid-Membrane-Incorporating Fullerenes Prepared by the Fullerene-Exchange Method. *Chemistry-an Asian Journal* 7, 605-613.
- Jeng, U., Lin, T.L., Shin, K., Hsu, C.H., Lee, H.Y., Wu, M.H., Chi, Z.A., Shih, M.C., Chiang, L.Y., 2003. Lipophilic C-60-derivative-induced structural changes in phospholipid layers. *Physica B-Condensed Matter* 336, 204-210.
- Jeng, U.S., Hsu, C.H., Lin, T.L., Wu, C.M., Chen, H.L., Tai, L.A., Hwang, K.C., 2005. Dispersion of fullerenes in phospholipid bilayers and the subsequent phase changes in the host bilayers. *Physica B-Condensed Matter* 357, 193-198.
- Jerebek, H., Pabst, G., Rappolt, M., Stockner, T., 2010. Membrane-mediated effect on ion channels induced by the anesthetic drug ketemine. *J.Am.Chem.Soc.* 132, 7990-7997.
- Li, L.W., Davande, H., Bedrov, D., Smith, G.D., 2007. A molecular dynamics simulation study of C-60 fullerenes inside a dimyristoylphosphatidylcholine lipid bilayer. *Journal of Physical Chemistry B* 111, 4067-4072.
- Li, Y., Chen, X., Gu, N., 2008. Computational Investigation of Interaction between Nanoparticles and Membranes: Hydrophobic/Hydrophilic Effect. *Journal of Physical Chemistry B* 112, 16647-16653.
- Lundbaek, J.A., Collingwood, S.A., Ingolfsson, H.I., Kapoor, R., Andersen, O.S., 2010. Lipid bilayer regulation of membrane protein function: gramicidin channels as molecular force probes. *Journal of the Royal Society Interface* 7, 373-395.
- Lyon, D.Y., Adams, L.K., Falkner, J.C., Alvarez, P.J.J., 2006. Antibacterial activity of fullerene water suspensions: Effects of preparation method and particle size. *Environmental Science & Technology* 40, 4360-4366.
- McIntosh, T.J., Simon, S.A., 1986. Hydration force and bilayer deformation: a reevaluation. *Biophys.J.* 25, 4058-4066.
- Monticelli, L., 2012. On Atomistic and Coarse-Grained Models for C-60 Fullerene. *Journal of Chemical Theory and Computation* 8, 1370-1378.
- Monticelli, L., Salonen, E., Ke, P.C., Vattulainen, I., 2009. Effects of carbon nanoparticles on lipid membranes: a molecular simulation perspective. *Soft Matter* 5, 4433-4445.
- Pabst, G., Katsaras, J., Raghunathan, V.A., Rappolt, M., 2003. Structure and interactions in the anomalous swelling regime of phospholipid bilayers. *Langmuir* 19, 1716-1722.
- Pabst, G., Rappolt, M., Amenitsch, H., Bernstorff, S., Laggner, P., 2000a. X-ray kinematography of temperature-jump relaxation probes the elastic properties of fluid bilayers. *Langmuir* 16, 8994-9001.
- Pabst, G., Rappolt, M., Amenitsch, H., Laggner, P., 2000b. Structural information from multilamellar liposomes at full hydration: full q-range fitting with high quality x-ray data. *Physical Review E* 62, 4000-4009.
- Petrache, H.I., Tristram-Nagle, S., Nagle, J.F., 1998. Fluid phase structure of EPC and DMPC bilayers. *Chem.Phys.Lipids* 95, 83-94.

- Prato, M., 1997. 60 Fullerene chemistry for materials science applications. *Journal of Materials Chemistry* 7, 1097-1109.
- Qiao, R., Roberts, A.P., Mount, A.S., Klaine, S.J., Ke, P.C., 2007. Translocation of C-60 and its derivatives across a lipid bilayer. *Nano Letters* 7, 614-619.
- Rappolt, M., 2010. Bilayer thickness estimations with “poor” diffraction data. *Journal of Applied Physics* 107, -.
- Rappolt, M., Laggner, P., Pabst, G., 2004. Structure and elasticity of phospholipid bilayers in the L α phase: A comparison of phosphatidylcholine and phosphatidylethanolamine membranes, In: Pandalai, S.G. (Ed.), *Recent Research Developments in Biophysics*. Transworld Research Network, Trivandrum, pp. 365-394.
- Rappolt, M., Pabst, G., 2008. Flexibility and structure of fluid bilayer interfaces, In: Nag, K. (Ed.), *Structure and dynamics of membranous interfaces*. John Wiley & Sons, Hoboken, pp. 45-81.
- Rappolt, M., Rapp, G., 1996. Simultaneous small- and wide-angle x-ray diffraction during the main transition of dimyristoylphosphatidylethanolamine. *Ber.Bunsenges.Phys.Chem.* 100, 1153-1162.
- Rossi, G., Barnoud, J., Monticelli, L., 2013. Partitioning and solubility of C60 fullerene in lipid membranes *Physica Scripta* 87, 058503.
- Ruoff, R.S., Tse, D.S., Malhotra, R., Lorents, D.C., 1993. Solubility of C-60 in a variety of solvents. *Journal of Physical Chemistry* 97, 3379-3383.
- Sayes, C.M., Fortner, J.D., Guo, W., Lyon, D., Boyd, A.M., Ausman, K.D., Tao, Y.J., Sitharaman, B., Wilson, L.J., Hughes, J.B., West, J.L., Colvin, V.L., 2004. The differential cytotoxicity of water-soluble fullerenes. *Nano Letters* 4, 1881-1887.
- Sayes, C.M., Gobin, A.M., Ausman, K.D., Mendez, J., West, J.L., Colvin, V.L., 2005. Nano-C-60 cytotoxicity is due to lipid peroxidation. *Biomaterials* 26, 7587-7595.
- Seelig, A., Seelig, J., 1974. The dynamic structure of fatty acyl chains in a phospholipid bilayer measured by deuterium magnetic resonance. *Biochemistry* 13, 4839-4845.
- Shinoda, W., DeVane, R., Klein, M.L., 2012. Computer simulation studies of self-assembling macromolecules. *Current Opinion in Structural Biology* 22, 175-186.
- Wang, I.C., Tai, L.A., Lee, D.D., Kanakamma, P.P., Shen, C.K.F., Luh, T.Y., Cheng, C.H., Hwang, K.C., 1999. C-60 and water-soluble fullerene derivatives as antioxidants against radical-initiated lipid peroxidation. *Journal of Medicinal Chemistry* 42, 4614-4620.
- Wong-Ekkabut, J., Baoukina, S., Triampo, W., Tang, I.M., Tieleman, D.P., Monticelli, L., 2008. Computer simulation study of fullerene translocation through lipid membranes. *Nature Nanotechnology* 3, 363-368.
- Zhang, R.T., Suter, R.M., Nagle, J.F., 1994. Theory of the structure factor of lipid bilayers. *Physical Review E* 50, 5047-5060.
- Zupanc, J., Drobne, D., Drasler, B., Valant, J., Iglic, A., Kralj-Iglic, V., Makovec, D., Rappolt, M., Sartori, B., Kogej, K., 2012. Experimental evidence for the interaction of C-60 fullerene with lipid vesicle membranes. *Carbon* 50, 1170-1178.

Figure captions

Fig. 1. Background subtracted SAXS data and corresponding fitted curves (solid lines). Data for A) pure POPC in dH₂O, B) POPC with 2 mol. % of C₆₀ and C) POPC with 10 mol. % of C₆₀ recorded at 25 °C are presented. (*Authors' remark: single column figure*).

Fig. 2. Membrane parameters, d (lattice spacing), d_{HH} (head-to headgroup distance), d_w (water layer thickness), and η (bending fluctuation) as a function of temperature in presence of dH₂O (red circles), 2 mol. % of C₆₀ (green triangles) and 10 mol. % of C₆₀ (blue squares). Note, that $d = d_{HH} + d_H + d_w$, with d_H being the headgroup extension. (*Authors' remark: single column figure*).

Fig. 3. Mean fluctuation of inter-membrane distance, σ , at 25 °C. (*Authors' remark: single column figure*).

Fig. 4. Electron density profiles and corresponding real space models: (A) Pure POPC bilayers in dH₂O, (B) POPC bilayers in presence of 2 mol. % of C₆₀, and (C) POPC bilayers with 10 mol. % of C₆₀. (*Authors' remark: 2-column figure*).

Fig. 5. Schemes of MLVs interacting with fullerenes: (A) Pure fluid bilayers get stabilized by adhering C₆₀ clusters, and (B) MLVs display homogeneously dissolved fullerenes in the hydrophobic core of the bilayers. The image displays a TEM micrograph of C₆₀ clusters (image taken with permission from ref. (Zupanc et al., 2012)). (*Authors' remark: 2-column figure*).

figure 1
[click here to download high resolution image](#)

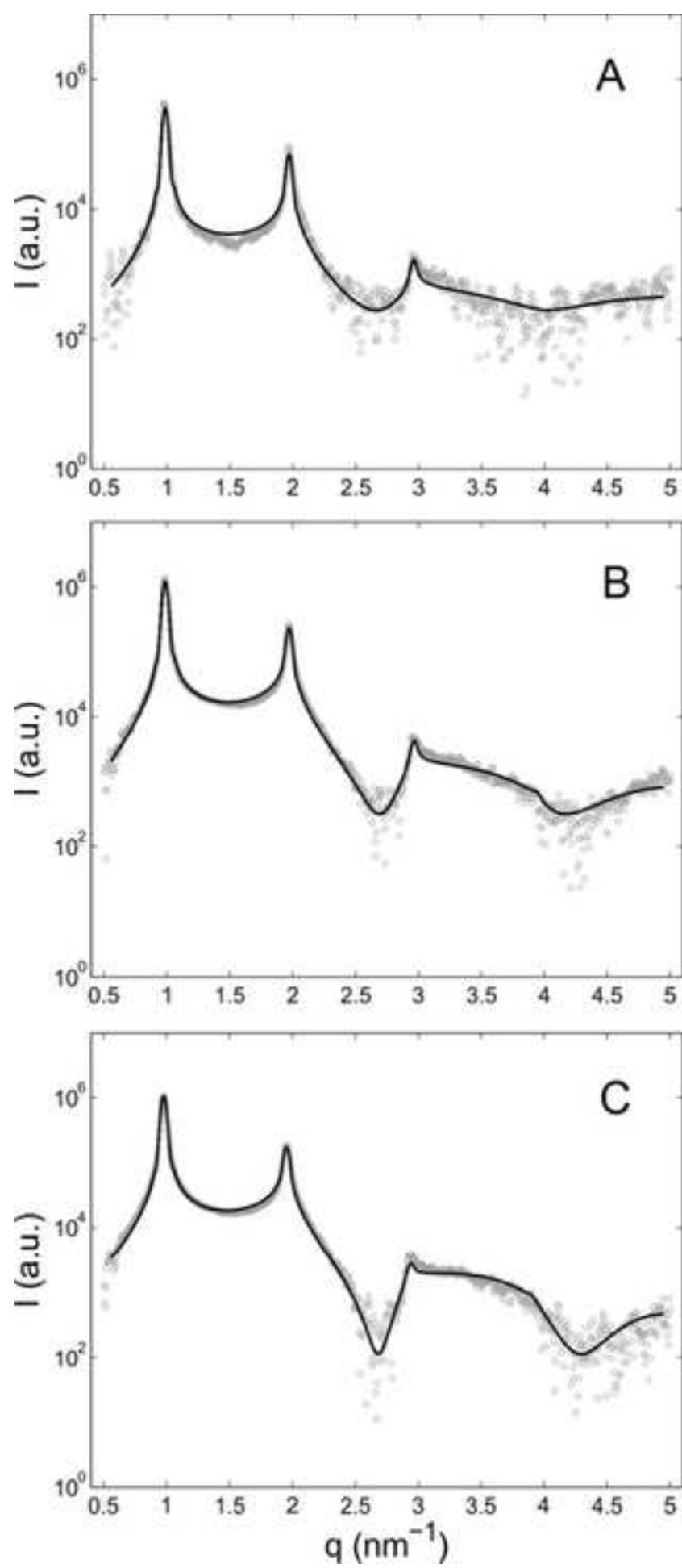


figure 2
[click here to download high resolution image](#)

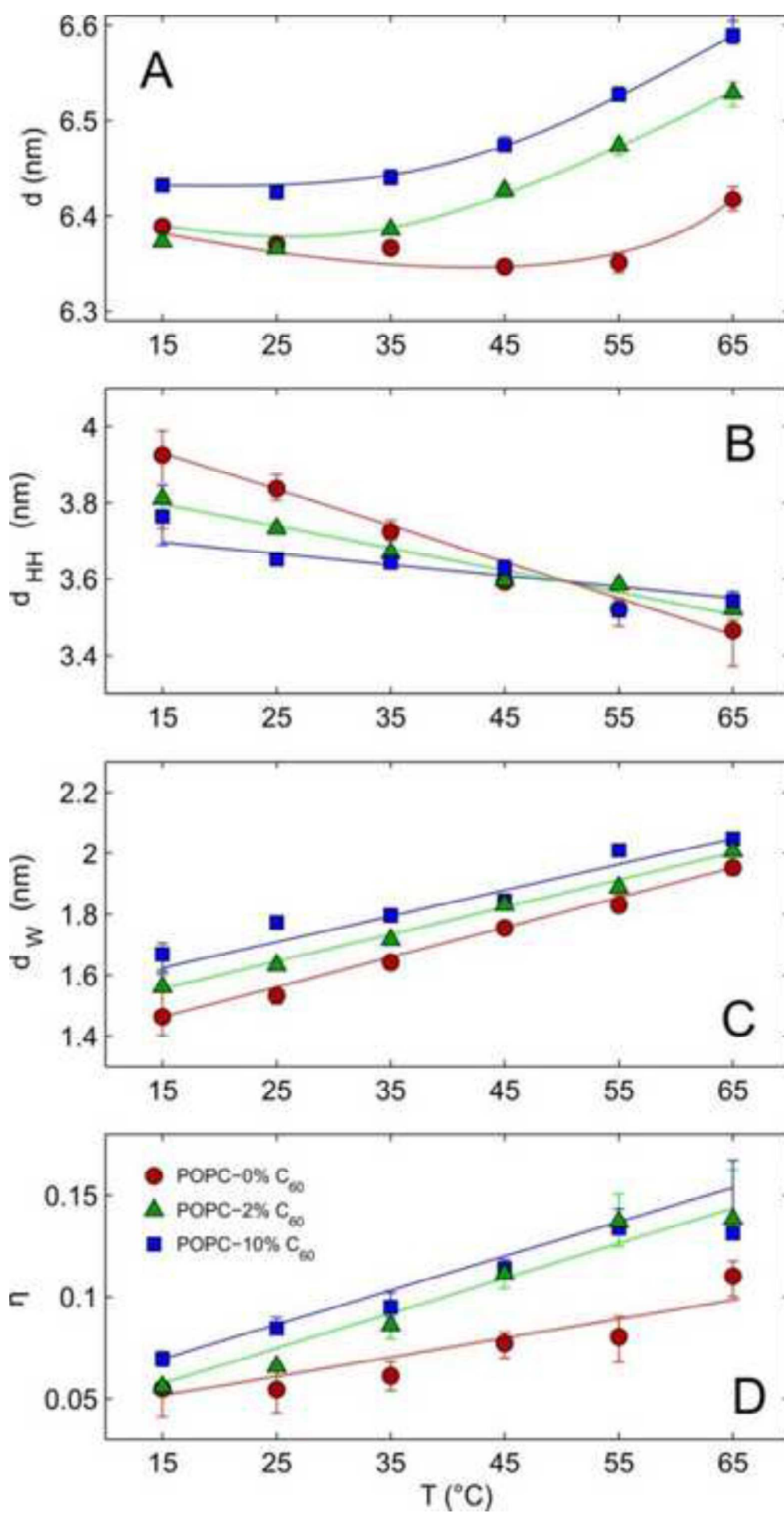


Figure 3
[Click here to download high resolution image](#)

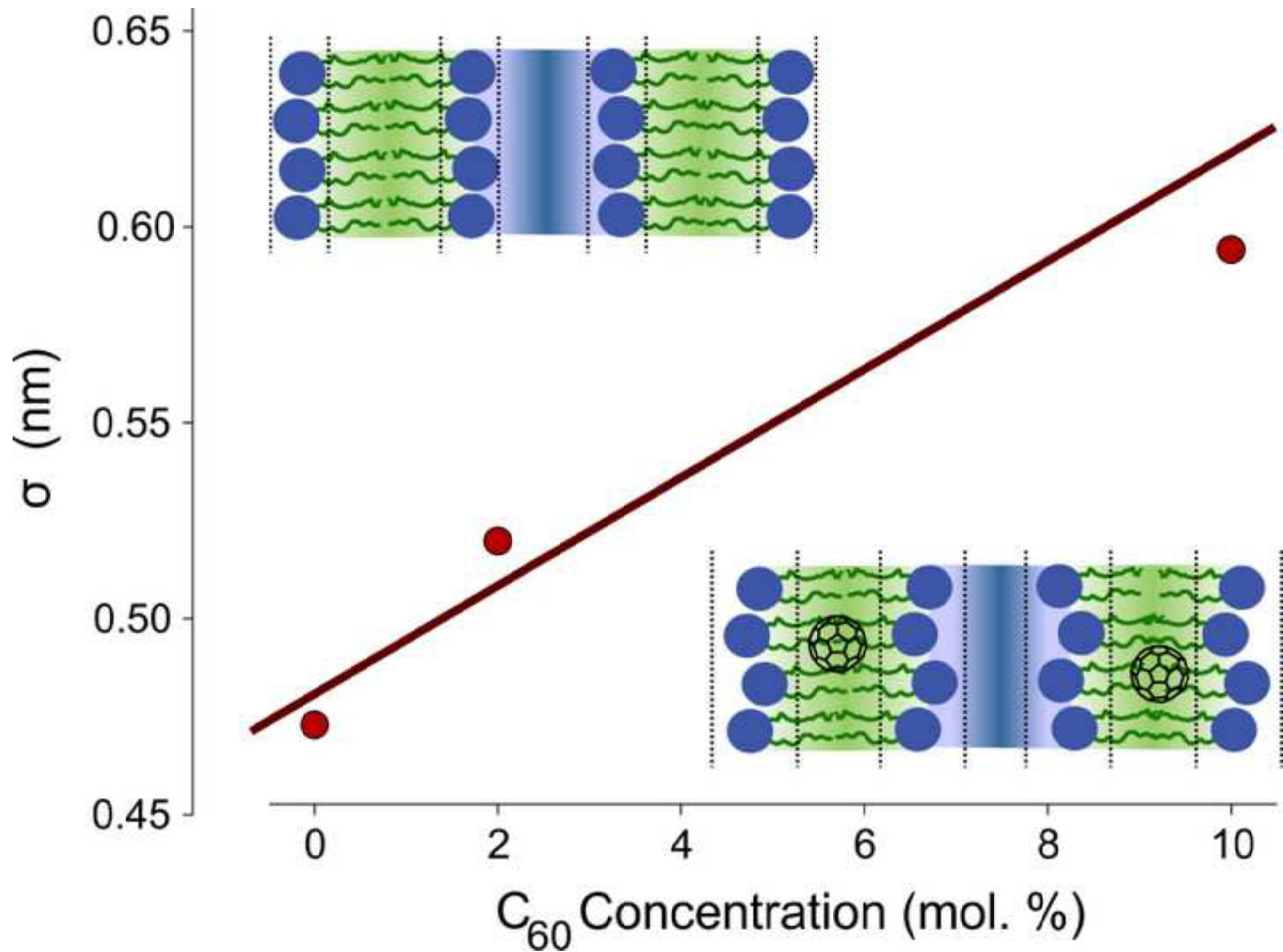
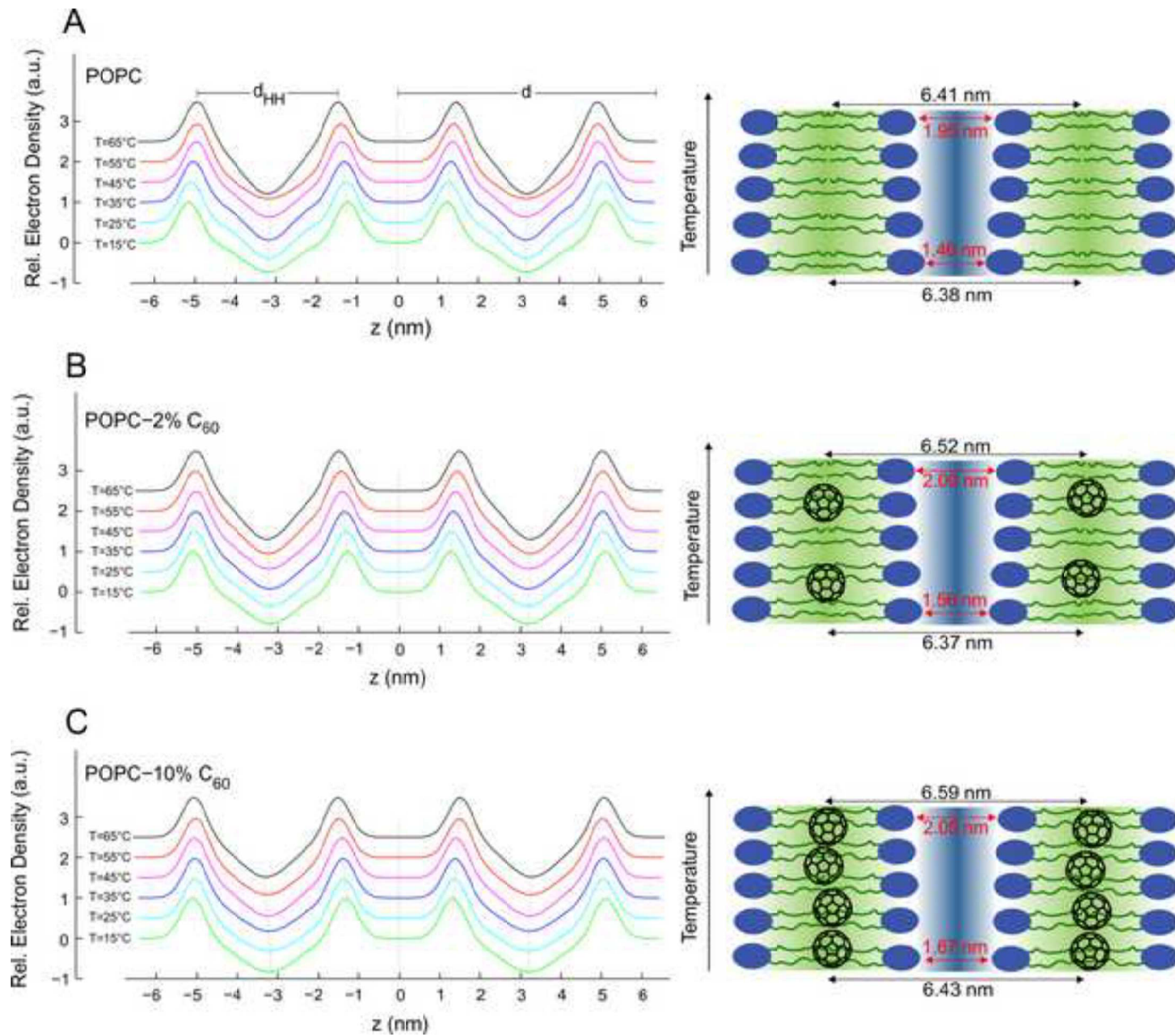
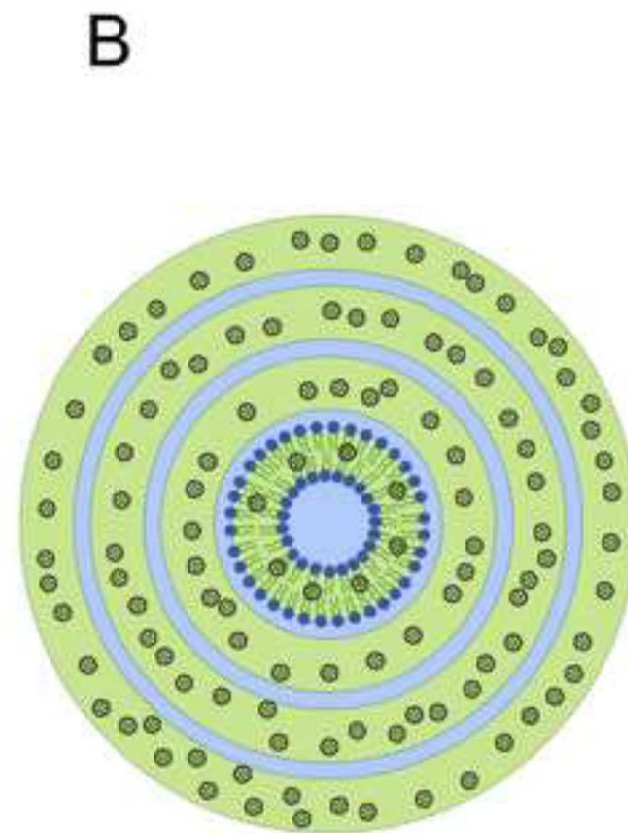
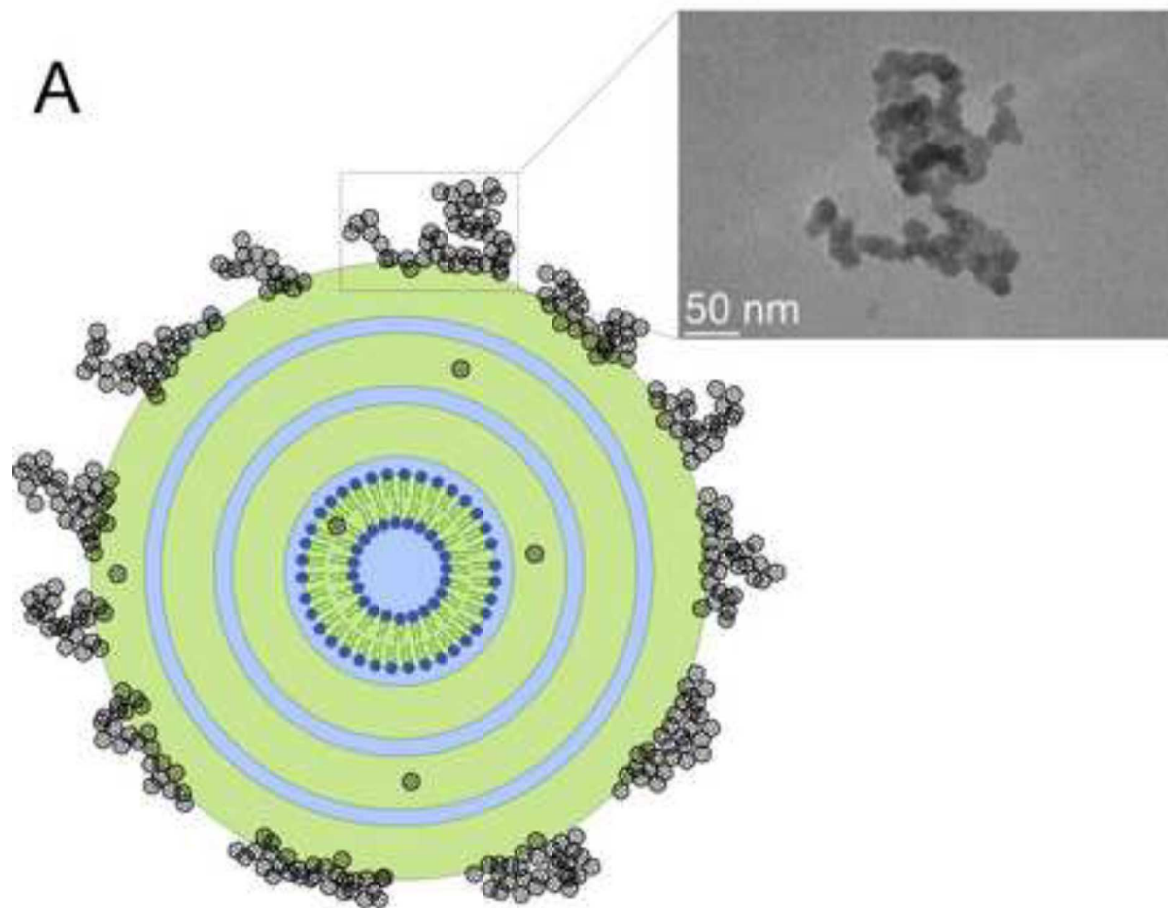


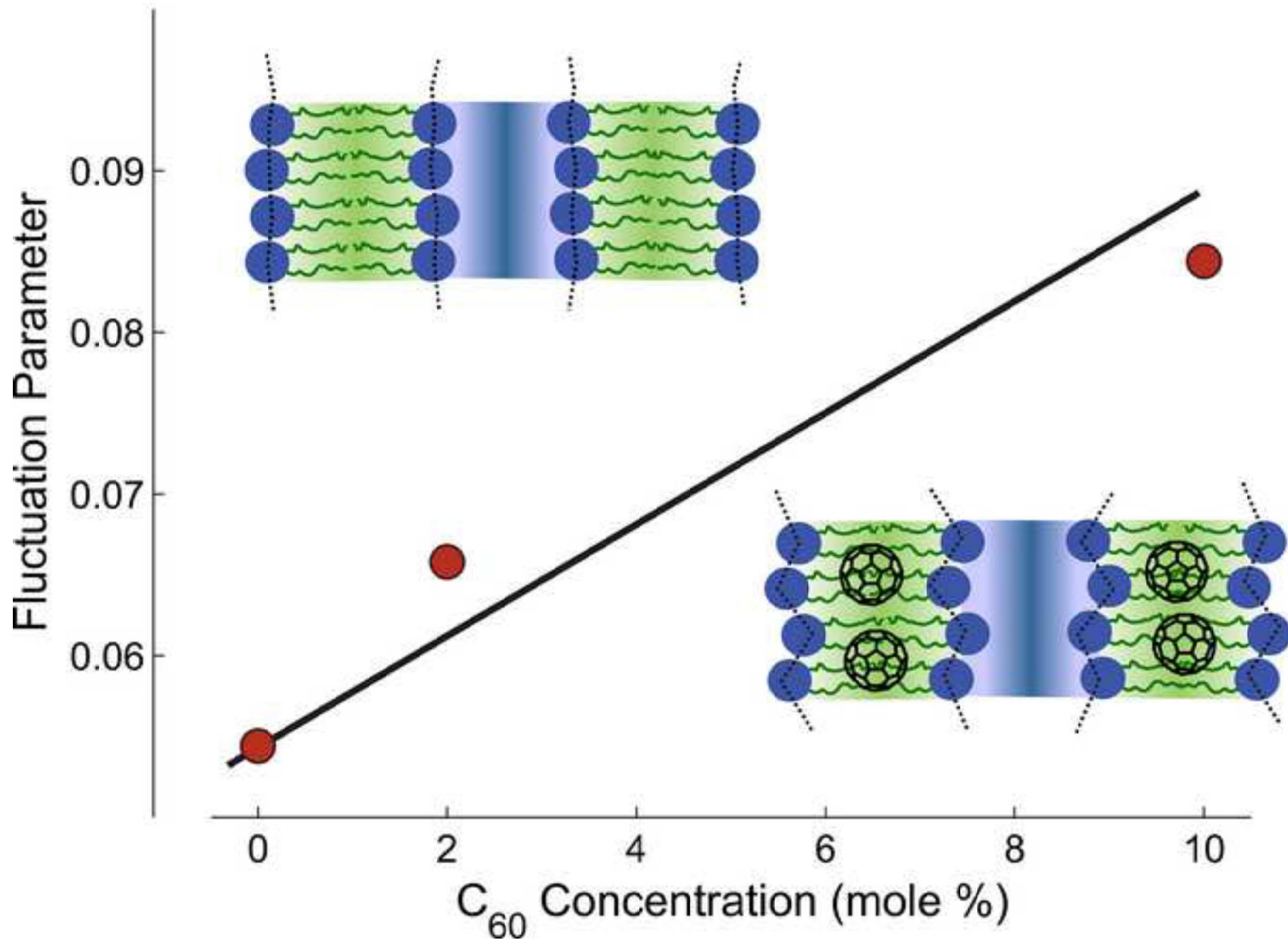
Figure 4

[Click here to download high resolution image](#)



Highlights

- Exposure to fullerenes (C_{60}) can lead to damaging effects on biomembranes.
- C_{60} causes increase in the bilayer undulations (~20 %).
- C_{60} enhances the mean inter-bilayer separation (~15%).
- C_{60} -incorporation increased the linear expansion coefficient.
- Addition of C_{60} causes a drop in the bending rigidity of the bilayers (20-40 %).

Increase of membrane fluctuation in presence of C_{60} 

Supplementary Material

Fullerene Up-Take Alters Bilayer Structure and Elasticity: A Small Angle X-ray Study

B. Drasler, D. Drobne, A. Sadeghpour, and M. Rappolt

Optimization method: The evolutionary computational technique of Particle Swarm Optimization (PSO) has been applied for the global fitting analysis ^{1,2} of the experimental X-ray scattering data. PSO is a modern optimization technique which is inspired by the social behaviour of flocks of birds or swarms of fish. Its algorithm is based on a population of candidate solutions, called particles, ‘flying’ through the problem space ^{3,4}. In our case, each particle is defined as a multi-dimensional vector with each index representing an input parameter of the fitting routine according to the modified Caillé theory ^{5,6}.

The optimization algorithm starts with a number of random particles (typically 500 solutions) generated from a given initial solution providing upper and lower limits. Through the algorithm the particles change their position with respect to their own previous best position, and the previous best position in the search space attained by any member. The particles converging speed can be controlled by an extra input parameter. The procedure continues until the positions of the particles remain relatively unchanged or until computational limitations are exceeded. To further improve of the goodness of the fit, the PSO algorithm was repeated several times, each time starting with neighbour solutions distributed around the best solution found so far. The goodness of each calculated curve was determined according to the reduced χ^2 :

$$\chi_v^2 = \frac{1}{N} \sum \frac{s^2}{\langle \sigma_i^2 \rangle},$$

where s^2 is the variance of the data set and σ_i is the uncertainty of each data point.

The errors were evaluated stepwise varying each parameter of the final solution until the reduced χ^2 deviates about 1 % from its determined value for the best fit.

The PSO algorithm ensures that the searching process will not be trapped in the local minima unlike the more traditional optimization algorithms. This guarantees the convergence into the optimal solution irrespective of the initial input parameters. In addition and unlike the genetic and other heuristic methods, this optimization algorithm has the advantage of executing a constrained solution space exploration which overcomes the problem of convergence into the premature solution ⁴.

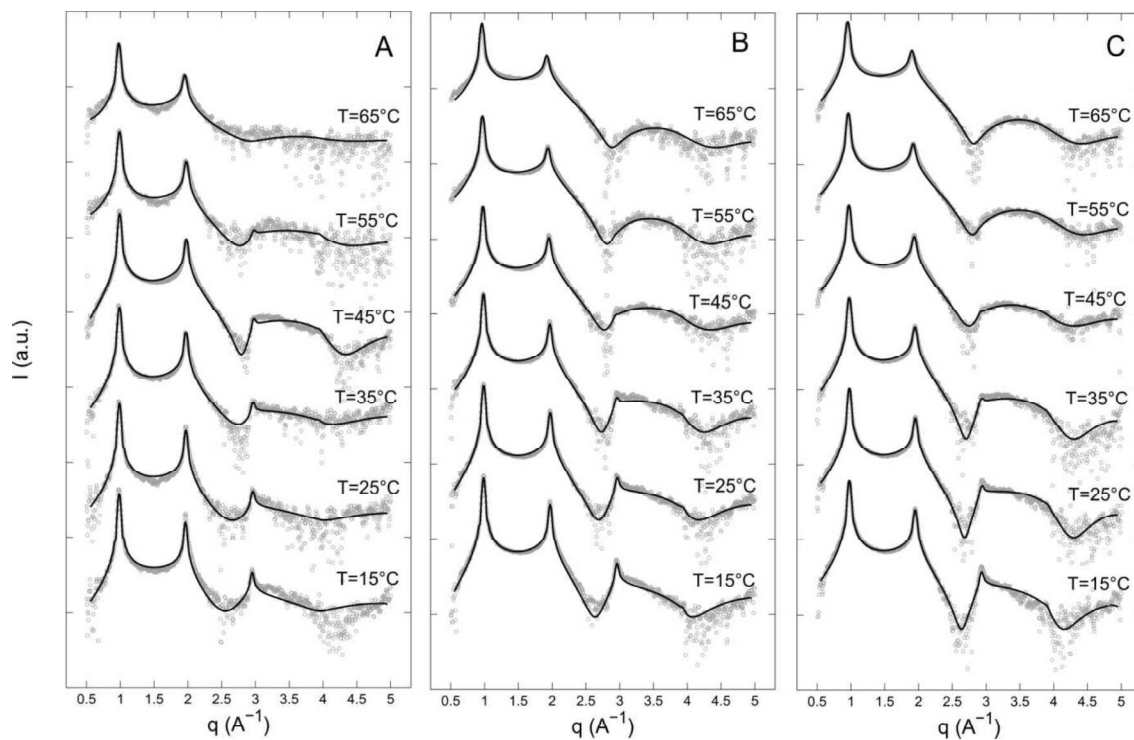


Fig. 1. The background subtracted scattering profiles and the corresponding fitted curves applying a global fitting analysis^{1,2} are presented for A) pure POPC in dH₂O, B) POPC with 2 mol. % C₆₀ and C) POPC with 10 mol. % of C₆₀ at different temperatures

References

1. G. Pabst, M. Rappolt, H. Amenitsch and P. Laggner, *Physical Review E*, 2000, **62**, 4000-4009.
2. M. Rappolt and G. Pabst, in *Structure and dynamics of membranous interfaces*, ed. K. Nag, John Wiley & Sons, Hoboken 2008, ch. 3, pp. 45-81.
3. J. Kennedy, R. Eberhart and Ieee, *Particle swarm optimization* 1995.
4. S. A. H. Soliman and A. A. H. Mantawy, Springer, New York 2012, pp. 1-414.
5. R. Zhang, R. M. Suter and J. F. Nagle, *Phys.Rev.E*, 1994, **50**, 5047-5060.
6. A. Caillé, *C.R.Acad.Sc.Paris B*, 1972, **274**, 891-893.

Supplementary Material

Fullerene Up-Take Alters Bilayer Structure and Elasticity: A Small Angle X-ray Study

B. Drasler, D. Drobne, A. Sadeghpour, and M. Rappolt

Optimization method: The evolutionary computational technique of Particle Swarm Optimization (PSO) has been applied for the global fitting analysis ^{1,2} of the experimental X-ray scattering data. PSO is a modern optimization technique which is inspired by the social behaviour of flocks of birds or swarms of fish. Its algorithm is based on a population of candidate solutions, called particles, ‘flying’ through the problem space ^{3, 4}. In our case, each particle is defined as a multi-dimensional vector with each index representing an input parameter of the fitting routine according to the modified Caillé theory ^{5,6}.

The optimization algorithm starts with a number of random particles (typically 500 solutions) generated from a given initial solution providing upper and lower limits. Through the algorithm the particles change their position with respect to their own previous best position, and the previous best position in the search space attained by any member. The particles converging speed can be controlled by an extra input parameter. The procedure continues until the positions of the particles remain relatively unchanged or until computational limitations are exceeded. To further improve of the goodness of the fit, the PSO algorithm was repeated several times, each time starting with neighbour solutions distributed around the best solution found so far. The goodness of each calculated curve was determined according to the reduced χ^2 :

$$\chi_v^2 = \frac{1}{N} \sum \frac{s^2}{\langle \sigma_i^2 \rangle},$$

where s^2 is the variance of the data set and σ_i is the uncertainty of each data point.

The errors were evaluated stepwise varying each parameter of the final solution until the reduced χ^2 deviates about 1 % from its determined value for the best fit.

The PSO algorithm ensures that the searching process will not be trapped in the local minima unlike the more traditional optimization algorithms. This guarantees the convergence into the optimal solution irrespective of the initial input parameters. In addition and unlike the genetic and other heuristic methods, this optimization algorithm has the advantage of executing a constrained solution space exploration which overcomes the problem of convergence into the premature solution ⁴.

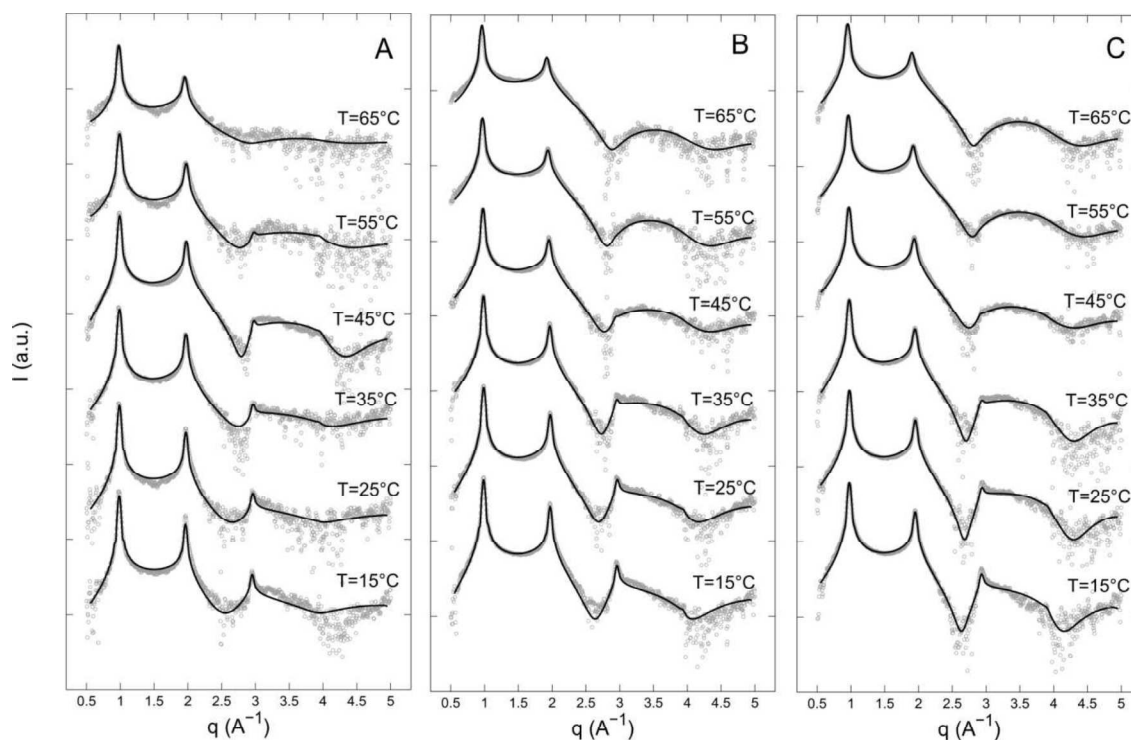


Fig. 1. The background subtracted scattering profiles and the corresponding fitted curves applying a global fitting analysis ^{1,2} are presented for A) pure POPC in dH₂O, B) POPC with 2 mol. % C₆₀ and C) POPC with 10 mol. % of C₆₀ at different temperatures

References

1. G. Pabst, M. Rappolt, H. Amenitsch and P. Laggner, *Physical Review E*, 2000, **62**, 4000-4009.
2. M. Rappolt and G. Pabst, in *Structure and dynamics of membranous interfaces*, ed. K. Nag, John Wiley & Sons, Hoboken 2008, ch. 3, pp. 45-81.
3. J. Kennedy, R. Eberhart and Ieee, *Particle swarm optimization* 1995.
4. S. A. H. Soliman and A. A. H. Mantawy, Springer, New York 2012, pp. 1-414.
5. R. Zhang, R. M. Suter and J. F. Nagle, *Phys.Rev.E*, 1994, **50**, 5047-5060.
6. A. Caillé, *C.R.Acad.Sc.Paris B*, 1972, **274**, 891-893.